

Angular-Momentum Effects on Neutron Emission by Dy and Tb Compound Nuclei*

GABRIEL N. SIMONOFF†† AND JOHN M. ALEXANDER‡

Lawrence Radiation Laboratory, University of California, Berkeley, California

(Received 7 June 1963)

We have studied as a function of energy three reactions producing 4.1-h Tb^{149g} from Tb compound nuclei and nine reactions producing Dy products from Dy compound nuclei. Incident particles were B^{10} , B^{11} , C^{12} , and O^{16} of energy 4 to 10.4 MeV per amu. Measurements of the average recoil range give strong evidence that all these reactions proceed by compound-nucleus formation. We report angular distributions of the final heavy products for all these reactions. From angular-distribution data we deduce the average total energies of photons and neutrons for each reaction. In the Tb reactions the average total photon energy is always less than 12 MeV. In the Dy reactions the average total photon energy varies linearly with total available energy from nearly 0 to about 30 MeV. These large differences in total photon energy are attributed to differences in the angular momenta of the initial compound nuclei. The rate of increase of the average kinetic energy of all neutrons (from Dy systems) is approximately proportional to the square root of the excitation energy. The relationships between total photon (or neutron) energy and total available energy seem to be independent of the average angular momentum of all compound nuclei. These relationships vary systematically with the number of emitted neutrons.

I. INTRODUCTION

IN this paper, we attempt to gain information on the average energies of neutrons and photons emitted from compound nuclei excited to energies up to approximately 125 MeV. We attempt to separate effects of angular momentum (J) from effects of excitation energy (E) by the comparison of compound nuclei having similar values of Z , A , and E but different values of J . The products Dy^{149} , Dy^{150} , and Dy^{151} were observed from the compound systems ${}_{66}Dy^{154}$ (formed by $C^{12}+Nd^{142}$), and Dy^{156} (formed by two reactions, $C^{12}+Nd^{144}$ and $O^{16}+Ce^{140}$). Also, the product Tb^{149g} has been observed from several Tb compound nuclei. Cross-section data imply that the latter reactions proceed from compound systems with $J \lesssim 7.5\hbar$,¹ whereas the former reactions involve much higher average angular momenta.²

In this work and in previous studies average range measurements have been used to test the reaction mechanism.³ These measurements give strong evidence that the reactions we study are reactions in which the neutrons are emitted with angular distributions symmetric about 90° .

We report angular-distribution measurements for the products previously mentioned. A relationship between total neutron energy and root-mean-square angle has been derived. This relationship assumes isotropic neutron emission but is not extremely sensitive to this

assumption. Using this relationship and our angular-distribution measurements, we obtain average total neutron energies and total photon energies associated with each individual reaction. In the preceding paper⁴ that presents cross section data we discuss the over-all energy and angular-momentum balance for these reactions.

We conclude that the low-spin Tb compound nuclei that decay to Tb^{149g} dissipate less than about 12 MeV in photons. The amount of photon emission from Dy compound nuclei of higher spin is quite different. This qualitative result was previously obtained by Morton, Choppin, and Harvey.⁵ Mollenauer has reported observations of photons emitted in complex nuclear reactions.⁶ His results also indicate that total photon energies increase with increasing J of the compound nucleus. Our results imply that total photon energies up to about 30 MeV are associated with neutron emission from Dy compound nuclei. The average kinetic energy of the emitted neutrons is approximately proportional to \sqrt{E} . The average total photon energy increases with increasing E or J , or both.

II. RECOIL EFFECTS OF THE COMPOUND-NUCLEUS MECHANISM

The basic features of the compound-nucleus mechanism are the following. A projectile and a target nucleus interact to form an excited compound system having a mean life that is long compared with the time required for the projectile to traverse the nuclear diameter. The excited compound nucleus decays by emitting particles and photons until a stable or radioactive final product is formed. The angular distribution of the emitted particles

* Work done under the auspices of the U. S. Atomic Energy Commission.

† On leave from Laboratoire Joliot Curie de Physique Nucléaire Orsay, France.

‡ Present address: Nouvelle Faculté des Sciences de Bordeaux, Talence (Gironde) France.

§ Present address: Department of Chemistry, State University of New York at Stony Brook, Stony Brook, New York.

¹ J. M. Alexander and G. N. Simonoff, Phys. Rev. **130**, 2383 (1963).

² T. D. Thomas, Phys. Rev. **116**, 703 (1959).

³ J. M. Alexander and L. Winsberg, Phys. Rev. **121**, 529 (1961); J. M. Alexander and D. H. Sisson, *ibid.* **128**, 2288 (1962).

⁴ J. M. Alexander and G. N. Simonoff, preceding paper, Phys. Rev. **132**, B93 (1963).

⁵ J. R. Morton, III, G. R. Choppin, and B. G. Harvey, Phys. Rev. **128**, 265 (1962).

⁶ J. F. Mollenauer, Phys. Rev. **127**, 867 (1962).

or photons is symmetric about $\pi/2$ in the frame of reference of the compound nucleus if the level density of the residual nucleus is large enough to justify the random-phase approximation.⁷ In this work we study systems with initial excitation energies of about 50 to 125 MeV, and thus we assume that this approximation is justified.

Let us consider in detail the consequences of this mechanism for two recoil properties of the final products: (a) range-straggling parameter ρ , and (b) root-mean-square angle (laboratory system), $\langle\theta_L^2\rangle^{1/2}$. Let \mathbf{v} denote the velocity given to the compound nucleus by the initial impact of the projectile (this is identical to the velocity of the center of mass). Let \mathbf{V} denote the velocity in the c.m. system given to the final product by the evaporation of particles. Let θ denote the c.m. angle between \mathbf{v} and \mathbf{V} and let θ_L denote the lab angle between \mathbf{v} and $\mathbf{v}+\mathbf{V}$. The angular distribution of \mathbf{V} is designated by $W(\theta)$, and the recoil range is taken as equal to $k|\mathbf{v}+\mathbf{V}|^N$, where k and N are constants. The projection R of the actual recoil ranges on the beam direction is given by $R=k|\mathbf{v}+\mathbf{V}|^N \cos\theta_L$.

If the average quantity $\langle V^2 \rangle$ is much less than v^2 , and if $W(\theta)$ is symmetric about $\pi/2$, then the average projection of the ranges on the beam direction, R_0 , can be considered to depend only on v , k , and N —and to be independent of V and $W(\theta)$.⁸ The average range R_0 of the product should be associated with a recoil energy E_R such that

$$E_R = \frac{E_b A_b A_R}{(A_b + A_T)^2}, \quad (1)$$

where mass number is denoted by A , with subscript b indicating the bombarding particle, subscript R the recoil atom or final product, and subscript T the target. The kinetic energy of the projectile in the laboratory system is denoted by E_b .

The contribution to the measured range straggling from the distribution of $\mathbf{v}+\mathbf{V}$ is given by

$$\langle (R-R_0)^2 \rangle = \frac{1}{2} \int_0^\pi [R(v, V, \theta) - R_0(v, V)]^2 W(\theta) \sin\theta d\theta. \quad (2)$$

This integral has been evaluated by substituting the appropriate functions of velocity for R and R_0 . For $V \ll v$, and for $W(\theta)=1$ we have, to order $(V/v)^3$,

$$\langle (R-R_0)^2 \rangle / R_0^2 = N^2 \langle V^2 \rangle / 3v^2; \quad (3)$$

for $W(\theta) = a + b \cos^2\theta$,

$$\frac{\langle (R-R_0)^2 \rangle}{R_0^2} = \frac{N^2 \langle V^2 \rangle [1 + (3b/5a)]}{3v^2 [1 + (b/3a)]}; \quad (4)$$

and for $W(\theta)$ proportional to $1/\sin\theta$,

$$\langle (R-R_0)^2 \rangle / R_0^2 = N^2 \langle V^2 \rangle / 2v^2. \quad (5)$$

Detailed calculations by the Monte Carlo method have shown that for $V^2 \ll v^2$ the range distribution due to evaporation effects can be closely approximated by a Gaussian distribution with straggling parameter denoted by ρ_n .⁹ Thus, we have

$$\rho_n^2 = \langle (R-R_0)^2 \rangle / R_0^2. \quad (6)$$

The average square of the angle $\langle\theta_L^2\rangle$ of the recoil atoms is given by

$$\langle\theta_L^2\rangle = \frac{1}{2} \int_0^\pi \left\{ \tan^{-1} \left(\frac{V \sin\theta}{v + V \cos\theta} \right) \right\}^2 W(\theta) \sin\theta d\theta. \quad (7)$$

To order $(V/v)^3$ for $W(\theta)=1$, we have

$$\langle\theta_L^2\rangle = 2 \langle V^2 \rangle / 3v^2. \quad (8)$$

For $W(\theta) = a + b \cos^2\theta$, we have

$$\langle\theta_L^2\rangle = \frac{2 \langle V^2 \rangle [1 + (b/5a)]}{3v^2 [1 + (b/3a)]}. \quad (9)$$

For $W(\theta)$ proportional to $1/\sin\theta$ we have

$$\langle\theta_L^2\rangle = \langle V^2 \rangle / 2v^2. \quad (10)$$

The equations given above show relationships between some observable properties and the magnitude of the velocities \mathbf{v} and \mathbf{V} . The velocity \mathbf{v} is, of course, specified by the momentum of the projectile and the mass of the compound nucleus:

$$v^2 = 2A_b E_b / (A_b + A_T)^2. \quad (11)$$

The value of $\langle V^2 \rangle$ is determined by the average total kinetic energy T_n of the emitted particles in the c.m. system and by their angular and energy distributions. The recoil velocity due to emission of photons can be neglected.

Assume that the compound nucleus emits nucleons in random directions then $W(\theta)=1$, and we have $\langle V^2 \rangle = \sum_{i=1}^x V_i^2$, where V_i is the additional recoil velocity due to the emission of the i th neutron and x is the total number of emitted neutrons. Then for $A_R \geq 20$ we obtain

$$\langle V^2 \rangle \approx 8T_n / (A_T + A_b + A_R)^2. \quad (12)$$

The total energy available in the c.m. system is $E_{c.m.} + Q$, therefore, the average total energy emitted as photons T_γ is

$$T_\gamma = E_{c.m.} + Q - T_n. \quad (13)$$

⁷ D. C. Peaslee, *Ann. Rev. Nucl. Sci.* **5**, 99 (1955); T. Ericson, *Advances in Physics*, edited by N. F. Mott (Taylor and Francis, Ltd., London, 1960), Vol. 9, p. 425.

⁸ L. Winsberg and J. M. Alexander, *Phys. Rev.* **121**, 518 (1961).

⁹ J. M. Alexander, L. Altman, and S. Howry, Lawrence Radiation Laboratory (unpublished calculations).

Thus, from Eqs. (3), (6), (11), and (12) we have

$$\rho_n^2 = \frac{4N^2 T_n (A_b + A_T)^2}{3E_b A_b (A_b + A_T + A_R)^2}, \quad (14)$$

and from Eqs. (8), (11), and (12) we have

$$\langle \theta_L^2 \rangle = \frac{(8T_n)(A_b + A_T)^2}{(3E_b A_b)(A_b + A_T + A_R)^2}. \quad (15)$$

In all these relationships the neutron mass is taken as unity.

If the angular distribution of the emitted particles is not isotropic, the development is much more complicated. However, from Eqs. (5) and (10), one can see that even an extreme case of $W(\theta) \propto 1/\sin\theta$ leads to changes of only about 22% in ρ_n , and about 13% in $\langle \theta_L^2 \rangle^{1/2}$.

III. EXPERIMENTAL TECHNIQUES AND RESULTS

In our experiments we have made observations of the nuclides 4.1-h Tb^{149g}, 7.4-min Dy¹⁵⁰, and 17.9-min Dy¹⁵¹. These are the only known alpha-emitting nuclides in the rare-earth region that have convenient decay periods and favorable alpha branching ratios. Therefore, measurement of the alpha radioactivity by ionization chambers allows us to identify these specific products without chemical analysis, thus eliminating chemical-yield errors.

In other work we have observed that cross sections for Tb^{149g} from Tb compound nuclei are very small.¹ Also, Dy¹⁵⁰ and Dy¹⁵¹ cross sections from Dy compound nuclei are very large.⁴ The excitation functions for Dy¹⁴⁹+Tb^{149g} from Dy compound nuclei closely resemble those for Dy¹⁵⁰ and Dy¹⁵¹.⁴ We infer that a dominant fraction of the Tb^{149g} that is observed from Dy compound nuclei actually comes from radioactive decay of Dy¹⁴⁹ to Tb^{149g}. Therefore, we refer to the recoil properties of Tb^{149g} produced from Dy compound systems as those of Dy¹⁴⁹.

A. Range Measurements

The range measurements were made with thin targets (30 to 100 $\mu\text{g}/\text{cm}^2$), and thin Al catcher foils (approximately 150 $\mu\text{g}/\text{cm}^2$), as described previously.^{3,8} On a probability scale, F_t , the fraction of the total activity that passed through catcher foils of combined thickness t , was plotted against t . These probability plots always indicate that the range distribution can be described as a Gaussian function with two parameters (the average range R_0 and the straggling parameter ρ):

$$P(R)dR = \frac{1}{R_0 \rho (2\pi)^{1/2}} \exp \left[-\frac{(R - R_0)^2}{\sqrt{2} R_0 \rho} \right] dR. \quad (16)$$

The results of the range measurements are given in

TABLE I. Range measurements in Al.

Reaction	Bombarding energy E_b (lab) (MeV)	Observed product	Average range R_0 (mg/cm ²)	Measured straggling parameter ρ	Nuclear reaction straggling parameter ρ_n^*	
Ce ¹⁴⁰ +O ¹⁶	146.0	Tb ¹⁴⁹	0.996	0.183	0.09 ± 0.035	
		Dy ¹⁵⁰	0.991	0.190	0.102 ± 0.03	
	140.0	Tb ¹⁴⁹	0.953	0.186	0.083 ± 0.04	
		Dy ¹⁵⁰	0.958	0.197	0.105 ± 0.03	
	128.1	Tb ¹⁴⁹	0.910	0.196	0.089 ± 0.033	
		Dy ¹⁵⁰	0.912	0.202	0.10 ± 0.03	
	Nd ¹⁴⁴ +C ¹²	112.4	Tb ¹⁴⁹	0.803	0.193	≈ 0
			Dy ¹⁵¹	0.758	0.200	≈ 0
		100.4	Dy ¹⁵¹	0.730	0.196	≈ 0
			Dy ¹⁵¹	0.677	0.199	≈ 0
100.0		Tb ¹⁴⁹	0.661	0.245	0.082 ± 0.03	
		Dy ¹⁵⁰	0.656	0.248	0.085 ± 0.03	
95.0	Tb ¹⁴⁹	0.549	0.224	≈ 0		
	Dy ¹⁵⁰	0.551	0.223	≈ 0		
	Dy ¹⁵¹	0.554	0.237	≈ 0		

* The value of ρ_n is given only if it is significantly different from zero.

Table I. The first three columns give the reaction, beam energy, and observed product, respectively. The values of the measured quantities R_0 and ρ are given in the fourth and fifth columns. The measured straggling parameter is the result of contributions from several sources: (a) finite target thickness ρ_w , (b) catcher-foil inhomogeneities ρ_f , (c) inherent straggling in the stopping process ρ_s , and (d) the nuclear reaction ρ_n . If all these contributions are treated as Gaussian we have

$$\rho_n^2 = \rho^2 - \rho_w^2 - \rho_f^2 - \rho_s^2. \quad (17)$$

The effects of ρ_w , ρ_f , and ρ_s have been subtracted as previously described,³ and we show the values of ρ_n in the last column.

The values of ρ_n are not accurate enough to specify T_n values from Eq. (14). We can only say that the values of ρ_n are not inconsistent with any conclusions deduced from the angular-distribution results. As shown in Eqs. (14) and (15), the values of ρ_n and $\langle \theta_L^2 \rangle^{1/2}$ are both related to T_n . The major result from the range measurements is the determination of the average range R_0 .

B. Angular-Distribution Measurements

The angular-distribution measurements were performed by essentially the same method as developed by Harvey *et al.*^{5,10} A thin target layer was exposed to a collimated beam from the Berkeley Hilac. The Nd¹⁴², Nd¹⁴⁴, Nd¹⁴⁶, and Ce¹⁴⁰ targets were prepared from enriched isotopes obtained from the Oak Ridge National Laboratory. The enrichments were 97.4% Nd¹⁴², 97.3% Nd¹⁴⁴, 96.2% Nd¹⁴⁶, and 99.6% Ce¹⁴⁰. A thick (0.001-in.) Al catcher foil was placed at some distance from the target; and the catcher was cut into rings concentric about the beam.

The geometry of the apparatus is shown in Fig. 1. The angular resolution of the beam was defined by two $\frac{1}{16}$ -in. collimators to approximately 0.5° in some experiments.

¹⁰ P. F. Donovan, B. G. Harvey, and W. H. Wade, Phys. Rev. 119, 218, 225 (1960).

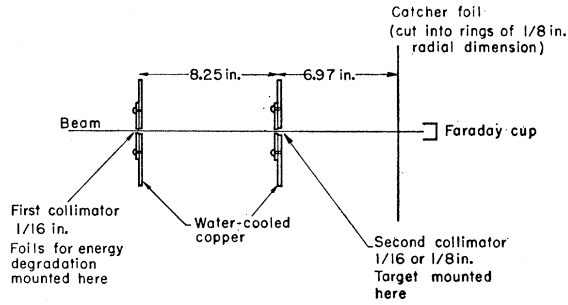


FIG. 1. Schematic diagram of the apparatus used for angular-distribution measurements.

In others the second collimator was $\frac{1}{8}$ in. in diameter, giving rise to an angular definition of approximately 1° . The effect of the size of the second collimator was measured experimentally (see Table III).

The catcher foil was cut by a stainless steel cutter and a hydraulic press into rings of $\frac{1}{8}$ -in. radial dimension. Each ring subtended approximately 1° . Two different cutters were used. The dimensions of these cutters were carefully calibrated by weighing several sets of rings cut from sheets of uniform Al foil. The angles defined by each ring are given in Table II.

TABLE II. Angles defined by each cutting edge (deg).^a

Ring number	Cutter 1	Cutter 2
	0	0
1	1.16	1.04
2	2.10	2.04
3	3.12	3.07
4	4.15	4.12
5	5.16	5.15
6	6.16	6.18
7	7.15	7.17
8	8.17	8.21
9	9.19	9.19
10	10.19	10.19
11	11.18	11.16
12	12.13	12.15
13	13.14	13.17
14	14.15	14.10
15	15.08	15.08
16	16.02	16.06

^a For each ring the inner and outer angles are given. The outer angle for any ring is the inner angle for the next.

The results of all angular-distribution measurements are given in Table III. The first two columns give the beam energy and target thickness, respectively. As shown in Table II, the two cutters had slightly different dimensions. Therefore, for each experiment we give the cutter, and, for each ring, the fractional cross section per unit angle $\Delta\sigma/\sigma\Delta\theta$. The average angle $\langle\theta_L\rangle$ was calculated by the relationship

$$\langle\theta_L\rangle = \sum_i (\Delta\sigma_i/\sigma) \langle\theta_i\rangle, \quad (18)$$

where $\langle\theta_i\rangle$ is the mean angle of the i th ring and $\Delta\sigma_i/\sigma$ is the fraction of the total activity observed in that ring. The root-mean-square angle was similarly calculated:

$$\langle\theta_L^2\rangle^{1/2} = [\sum_i (\Delta\sigma_i/\sigma) \langle\theta_i^2\rangle]^{1/2}, \quad (19)$$

where $\langle\theta_i^2\rangle$ is the mean-square angle of the i th ring. Values of $\Delta\sigma_i$ less than 2% of the maximum value of $\Delta\sigma_i$ were not included in the summations.

The effect of target thickness on the angular distribution of Tb^{149g} was carefully studied for several cases. One series of these experiments is shown in Fig. 2. The values of $\langle\theta_L\rangle$ and $\langle\theta_L^2\rangle^{1/2}$ change significantly but not very rapidly with the target thickness (see Fig. 3). We have used the values of $d\langle\theta_L\rangle/dW$ and $d\langle\theta_L^2\rangle^{1/2}/dW$ shown in Fig. 3 to correct these average properties to zero target thickness. The assumption was made that all reactions of the same projectile have the same value of $d\langle\theta_L\rangle/dW$ and $d\langle\theta_L^2\rangle^{1/2}/dW$. This is probably a very good approximation (especially for the C^{12} and O^{16} experiments), because the angular distributions and recoil velocities are very similar. The detailed angular distributions in Table III for $W=0$ were obtained by linearly extrapolating $\Delta\sigma/\sigma\Delta\theta$ to $W=0$ for each ring. This procedure becomes more uncertain, of course, with increasing angle.

The effect of collimator size was carefully studied for two different cases ($\text{Nd}^{144}+122.8\text{-MeV}$ and 77.5-MeV

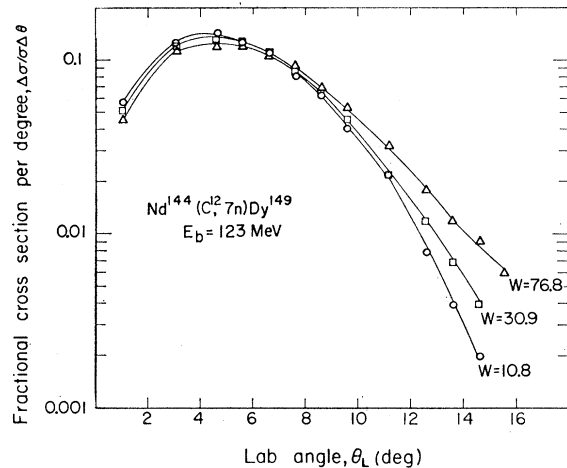


FIG. 2. The effect of target thickness on observed angular distribution. The target thickness W is denoted for each curve in $\mu\text{g}/\text{cm}^2$. These data are for the reaction $\text{Nd}^{144}+123\text{-MeV } \text{C}^{12} \rightarrow \text{Dy}^{149}+7n$.

TABLE III. Angular distribution results.

Bombarding energy, E_b (lab) (MeV)	Target thickness t ($\mu\text{g}/\text{cm}^2$)	Cutter	Fractional cross section per unit angle $\Delta\sigma/\sigma\Delta\theta$ (deg $^{-1}$)																(θ_L)	$(\theta_R)^{1/2}$						
			1	2	3	4	5	6	7	8	9	10	11	12	13	14	15	16			17	18				
			Pr ¹⁴¹ (C ¹² , ⁴ⁿ)Tb ^{149g}																							
>57.7 ^a	27.2	2 ^b	0.046	0.107	0.155	0.169	0.149	0.121	0.090	0.055	0.039	0.020	0.012	0.007	(0.004) ^c	(0.002)							4.51	5.15		
>59.9 ^a	30.3	1 ^b	0.044	0.108	0.149	0.155	0.151	0.128	0.096	0.065	0.040	0.024	0.016	0.008	(0.006)	(0.004)								4.69	5.35	
67.8	27.2	2 ^b	0.033	0.089	0.132	0.149	0.150	0.133	0.100	0.074	0.045	0.030	0.018	0.012	0.008	0.005								4.97	5.64	
70.1	30.3	2 ^b	0.033	0.079	0.126	0.147	0.144	0.132	0.111	0.083	0.050	0.037	0.019	0.008	0.007	(0.005)								5.09	5.73	
			Nd ¹⁴⁶ (B ¹⁰ , ⁷ⁿ)Tb ^{149g}																							
75.1	25.2	1 ^b	(0.031)	0.067	0.092	0.112	0.122	0.118	0.111	0.089	0.083	0.064	0.042	0.026	\leftarrow 0.016 \rightarrow	\leftarrow 0.002 \rightarrow								5.97	6.77	
102.4	25.2	2 ^b	(0.024)	0.035	0.049	0.069	0.079	0.096	0.098	0.098	0.090	0.082	0.062	0.067	\leftarrow 0.045 \rightarrow	\leftarrow 0.022 \rightarrow	(0.011)							7.78	8.64	
			Nd ¹⁴⁶ (B ¹¹ , ⁸ⁿ)Tb ^{149g}																							
90.2	27.4	2 ^b	(0.059)	0.078	0.095	0.114	0.126	0.122	0.101	0.088	0.062	0.056	0.034	0.019	0.012	0.008	(0.005)	(0.003)							5.54	6.37
103.7	27.4	2	(0.025)	0.047	0.073	0.099	0.104	0.122	0.109	0.112	0.074	0.075	0.051	0.037	0.028	0.013	0.010	(0.007)	(0.005)	(0.003)					6.69	7.53
103.7	89.0	1	(0.026)	0.046	0.069	0.090	0.099	0.108	0.101	0.096	0.081	0.071	0.057	0.043	0.037	0.023	0.017	(0.011)	(0.008)	(0.006)					7.13	8.07
103.7	0		0.025	0.048	0.074	0.100	0.107	0.113	0.111	0.110	0.078	0.075	0.048	0.034	0.024	0.008									6.50	7.29
112.8	27.4	1	(0.027)	0.043	0.067	0.083	0.101	0.113	0.108	0.094	0.085	0.075	0.053	0.044	0.036	0.025	0.013	(0.011)	(0.007)	(0.005)					7.13	8.04
			Nd ¹⁴⁶ (C ¹² , ³ⁿ)Dy ¹⁵¹																							
55.6	30.7	2 ^b	0.048	0.130	0.159	0.173	0.160	0.115	0.084	0.046	0.031	0.014	0.010	0.006											4.23	4.83
70.1	30.7	1 ^b	0.043	0.106	0.137	0.159	0.157	0.124	0.096	0.072	0.040	0.026	0.014	0.008	0.008										4.73	5.37
			Nd ¹⁴⁶ (C ¹² , ⁴ⁿ)Dy ¹⁵⁰																							
70.1	30.7	1 ^b	0.043	0.101	0.158	0.170	0.148	0.118	0.087	0.057	0.042	0.028	0.015	0.013	(0.009)										4.68	5.36
83.4	30.7	2 ^b	0.033	0.092	0.134	0.153	0.151	0.130	0.099	0.070	0.047	0.030	0.017	0.011	0.006	0.004									4.92	5.57
92.0	30.7	1 ^b	0.036	0.089	0.119	0.138	0.146	0.129	0.110	0.086	0.053	0.036	0.022	0.015	0.009	0.004									5.18	5.85
			Nd ¹⁴⁶ (C ¹² , ⁵ⁿ)Dy ¹⁴⁹																							
83.4	30.7	2 ^b	0.038	0.097	0.136	0.159	0.153	0.125	0.095	0.065	0.046	0.027	0.015	0.010	0.007	0.005									4.82	5.49
92.0	30.7	1 ^b	0.038	0.093	0.132	0.152	0.146	0.132	0.102	0.075	0.049	0.030	0.021	0.011	0.007	0.004									4.98	5.64
100.6	30.7	1 ^b	0.036	0.088	0.126	0.147	0.142	0.129	0.110	0.079	0.054	0.032	0.021	0.012	0.008	0.004									5.10	5.77
111.7	30.7	1 ^b	\leftarrow 0.053 \rightarrow	0.110	0.132	0.137	0.130	0.110	0.088	0.064	0.043	0.028	0.018	0.010	\leftarrow 0.005 \rightarrow										5.43	6.15
122.8	30.7	1 ^b	0.038	0.066	0.092	0.115	0.127	0.124	0.112	0.096	0.075	0.053	0.039	0.024	\leftarrow 0.013 \rightarrow	(0.004)									5.84	6.58
			Nd ¹⁴⁴ (C ¹² , ⁵ⁿ)Dy ¹⁵¹																							
77.5	77.0	2	0.036	0.086	0.123	0.140	0.137	0.115	0.096	0.074	0.052	0.038	0.025	0.018	0.015	0.011	(0.007)	(0.005)	(0.004)						5.39	6.26
77.5	77.0	1 ^b	0.039	0.080	0.116	0.139	0.127	0.119	0.101	0.076	0.054	0.041	0.027	0.021	0.015	0.014	(0.008)	(0.006)	(0.004)	(0.003)					5.63	6.56
83.4	30.9	2	0.040	0.100	0.135	0.149	0.140	0.117	0.105	0.075	0.047	0.029	0.014	0.013	0.010	(0.005)	(0.003)								4.94	5.66
94.0	30.9	1	0.050	0.089	0.114	0.129	0.133	0.137	0.101	0.080	0.059	0.037	0.024	0.013	0.010	(0.006)	(0.004)	(0.003)							5.25	5.88

TABLE III (continued).

Bombarding energy E_b (lab) (MeV)	Target thickness W ($\mu\text{g}/\text{cm}^2$)	Cutter	Fractional cross section per unit angle $\Delta\sigma/\sigma\Delta\theta$ (deg $^{-1}$)																$(\theta_L)^2$		
			1	2	3	4	5	6	7	8	9	10	11	12	13	14	15	16		17	18
			Nd ¹⁴⁴ (C ¹² ,6n)Dy ¹⁴⁰																		
94.0	30.9	1	0.048	0.088	0.114	0.146	0.149	0.117	0.099	0.072	0.048	0.037	0.027	(0.017)	(0.012)	(0.008)	(0.006)	(0.004)	5.24	6.04	
99.7	30.9	2	←0.054	→	←0.129	→	0.147	0.131	0.107	0.082	0.061	0.038	←0.014	→	0.012	0.006	(0.003)		5.22	5.93	
111.6	30.9	1	←0.049	→	←0.120	→	0.133	0.133	0.109	0.086	0.066	0.045	←0.024	→	0.012	0.008	0.005	(0.003)	5.56	6.33	
122.8	76.8	1	←0.044	→	←0.096	→	0.115	0.126	0.106	0.092	0.078	0.058	←0.037	→	0.029	0.016	0.012	0.005	6.24	7.09	
			Nd ¹⁴⁴ (C ¹² ,7n)Dy ¹⁴⁰																		
94.0	30.9	1	(0.054)	0.085	0.119	0.152	0.146	0.120	0.106	0.077	0.046	0.028	0.018	0.014	0.011	(0.006)	(0.004)		5.03	5.76	
99.7	30.9	2	←0.067	→	0.121	0.139	0.143	0.129	0.103	0.075	0.051	0.035	←0.016	→	0.008	0.006	(0.003)		5.05	5.80	
111.6	30.9	1	0.034	0.082	0.118	0.139	0.138	0.126	0.103	0.088	0.057	0.039	←0.020	→	0.012	(0.008)	(0.005)	(0.004)	5.40	6.15	
122.8	30.9	2 ^b	←0.047	→	←0.112	→	0.130	0.129	0.110	0.090	0.068	0.048	0.035	0.024	0.013	0.008	0.006	(0.004)	5.73	6.51	
122.8	10.8	1	←0.058	→	←0.125	→	0.141	0.126	0.110	0.084	0.063	0.040	←0.022	→	0.008	0.004	0.002		5.21	6.01	
122.8	30.9	2	←0.051	→	←0.121	→	0.135	0.126	0.111	0.086	0.065	0.046	←0.022	→	0.012	0.007	0.004		5.48	6.22	
122.8	76.8	1	←0.046	→	←0.111	→	0.120	0.122	0.105	0.091	0.069	0.053	←0.032	→	0.018	0.012	0.009	0.006	(0.004)	6.01	6.88
122.8	0		←0.057	→	←0.127	→	0.145	0.128	0.110	0.083	0.062	0.039	←0.018	→	0.007	0.003	0.0015		5.09	5.84	
			Ce ¹⁴⁰ (O ¹⁶ ,5n)Dy ¹⁴¹																		
89.7	36.4	2	0.062	0.142	0.187	0.188	0.167	0.100	0.063	0.030	0.014	0.010	0.006	0.006					3.85	4.40	
101.0	36.4	1	0.053	0.142	0.186	0.189	0.145	0.113	0.075	0.048	0.019	0.011	0.004	0.002					4.00	4.53	
111.0	21.0	2	0.045	0.129	0.177	0.184	0.159	0.120	0.079	0.043	0.020	0.011	0.005	0.002	0.001				4.08	4.70	
			Ce ¹⁴⁰ (O ¹⁶ ,6n)Dy ¹⁴⁰																		
101.0	36.4	1	0.063	0.134	0.166	0.183	0.167	0.120	0.079	0.024	0.032	0.008	0.008	0.004					4.03	4.59	
111.0	21.0	2	0.045	0.129	0.177	0.184	0.159	0.120	0.079	0.043	0.020	0.011	0.005	0.002	0.001				4.08	4.70	
121.1	36.4	2	0.047	0.114	0.151	0.177	0.166	0.131	0.080	0.054	0.040	0.021	0.013	0.006					4.44	5.06	
130.4	36.4	2	0.038	0.110	0.158	0.177	0.153	0.124	0.089	0.059	0.036	0.022	0.007	0.003					4.42	4.97	
139.2	21.0	2	0.040	0.108	0.164	0.171	0.160	0.120	0.094	0.055	0.033	0.019	0.008	0.003					4.37	4.92	
			Ce ¹⁴⁰ (O ¹⁶ ,7n)Dy ¹⁴⁰																		
111.0	21.0	2	0.043	0.120	0.161	0.172	0.158	0.120	0.086	0.055	0.030	0.016	0.007	0.005	0.002	0.0006			4.33	4.91	
111.0	72.8	1	0.043	0.107	0.150	0.163	0.153	0.126	0.094	0.064	0.037	0.022	0.013	0.007	0.005	0.004			4.64	5.28	
111.0	0		0.043	0.125	0.165	0.175	0.160	0.118	0.083	0.051	0.027	0.014	0.006	0.004	0.0004				4.20	4.76	
121.1	36.4	1	0.045	0.122	0.154	0.170	0.158	0.128	0.092	0.058	0.034	0.013	0.010	0.006					4.39	4.96	
130.4	36.4	1	0.047	0.114	0.157	0.169	0.156	0.125	0.093	0.058	0.035	0.020	0.008	0.007					4.43	5.01	
139.2	36.4	1	0.046	0.110	0.153	0.166	0.153	0.135	0.091	0.059	0.037	0.019	0.009	0.007	0.003				4.50	5.09	
139.2	21.0	2	0.043	0.113	0.157	0.171	0.156	0.127	0.088	0.061	0.033	0.018	0.008	0.004					4.38	4.95	
163.0	36.4	1	0.039	0.091	0.130	0.149	0.146	0.135	0.110	0.077	0.053	0.030	0.017	0.009	0.003				4.93	5.55	

^a The energy-degrading foils were damaged by the beam.

^b The second collimator was § in.

^c Values in parentheses were obtained by graphical extrapolation.

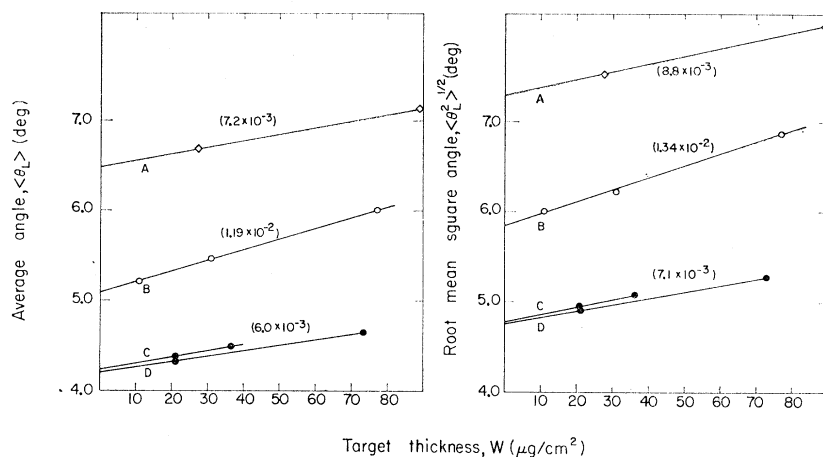


FIG. 3. The dependence of (a) the average angle $\langle \theta_L \rangle$ and (b) the root-mean-square angle $\langle \theta_L^2 \rangle^{1/2}$ on target thickness W . Curves A are for the reaction $\text{Nd}^{146} + 104\text{-MeV } \text{B}^{11} \rightarrow \text{Tb}^{149} + 8n$; B for $\text{Nd}^{144} + 123\text{-MeV } \text{C}^{12} \rightarrow \text{Dy}^{149} + 7n$; C for $\text{Ce}^{140} + 139\text{-MeV } \text{O}^{16} \rightarrow \text{Dy}^{149} + 7n$; D for $\text{Ce}^{140} + 111\text{-MeV } \text{O}^{16} \rightarrow \text{Dy}^{149} + 7n$. The numbers in parentheses denote the slopes of the lines in $\text{deg}/(\mu\text{g}/\text{cm}^2)$.

C^{12}). The angular distribution was measured with two $\frac{1}{8}$ -in. collimators (angular definition $\approx 0.5^\circ$) and in a separate experiment with the second collimator $\frac{1}{8}$ in. (angular definition $\approx 1^\circ$). The average angles $\langle \theta_L \rangle$ and $\langle \theta_L^2 \rangle^{1/2}$ were enlarged by 0.25 and 0.30° , respectively, by the poorer angular definition of the beam. We assume that no correction is necessary for experiments with two $\frac{1}{8}$ -in. collimators, and for the other experiments we correct the average angles by the above values. The corrected values of the average angles are given in Table IV along with average energies that are discussed later.

IV. DISCUSSION

A. Ranges

In preceding papers we have presented an internal-consistency argument for using average range values to test the validity of the compound-nucleus model.³ The lack of independent range-energy data for heavy-recoil atoms necessitates this consistency test. First, assume that the compound-nucleus mechanism is valid. Thus, Eq. (1) should give the recoil energy E_R , appropriate to the average range R_0 . Then the values of R_0 are plotted

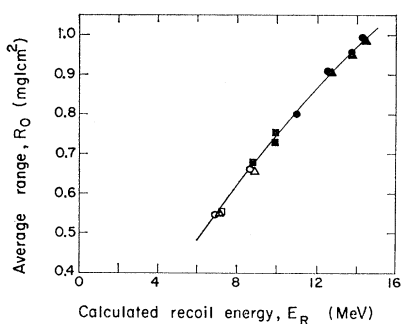


FIG. 4. Average range R_0 in Al versus the calculated recoil energy E_R . Symbols are as follows: Dy^{151} \square ; Dy^{150} \triangle ; Dy^{149} \circ . Open symbols are for the reactions $\text{C}^{12} + \text{Nd}^{144}$; closed, for $\text{O}^{16} + \text{Ce}^{140}$. The smooth curve is from Ref. 3.

versus E_R , as in Fig. 4. From this figure we see that one smooth curve fits all the measurements. Furthermore, this curve, which involves data for Dy^{150} and Dy^{151} , is identical with that for Tb^{149} range measurements from many other reactions.³ This test implies that Eq. (1) gives a correct description of the recoil energy or, in other words, that the projectile transfers all its momentum to the compound system. We conclude that the most likely mechanism for all these reactions is compound-nucleus formation, followed by emission of particles with forward-backward symmetry. All further discussion is based on this conclusion.

B. Angular Distributions

From the average recoil-range measurements we have concluded that, in all the reactions studied here, the angular distribution of the emitted neutrons is essentially symmetric about the $\pi/2$ plane in the center-of-mass system. We use measurements of the angular distribution of the final products to calculate the average kinetic energies of the neutrons and also average total photon energies.

The angular distribution of the final products depends on the energy and angular distributions of the emitted neutrons (see Sec. II). If the neutrons are emitted only as s waves, then their emission is isotropic. However, if neutrons are emitted with nonzero l values, then forward-backward peaking is expected.⁷ The classical limit to this forward-backward preference is given by an angular distribution of the form $W(\theta) \propto 1/\sin\theta$. Experimental studies of heavy-ion reactions have shown that alpha particles and fission fragments are emitted with angular distributions approaching this limit; neutrons and protons are emitted with much less forward-backward peaking.¹¹ Ericson's formulation of this problem

¹¹ W. J. Knox, A. R. Quinton, and C. E. Anderson, Phys. Rev. **120**, 2120 (1960); H. C. Britt and A. R. Quinton, *ibid.* **120**, 1768 (1960); V. E. Viola, Jr., T. D. Thomas, and G. T. Seaborg, University of California Radiation Laboratory Report UCRL-10248, 1962 (unpublished); H. W. Broek, Phys. Rev. **124**, 233 (1961).

TABLE IV. Average angles and energies.

Bombarding energy (lab) E_b (MeV)	Corrected average angle $\langle\theta_L\rangle$ (deg)	Corrected root-mean-square angle $\langle\theta_L^2\rangle^{1/2}$ (deg)	Total available energy, $E_{a,m} + Q$ (MeV)	Average total neutron energy, T_n (MeV)	Average total photon energy, T_γ (MeV)
Pr ¹⁴¹ (C ¹² ,4n)Tb ^{149g}					
>57.7	3.94	4.49	>6.2	<6.2	>0.0
>59.9	4.08	4.64	>7.9	<6.8	>1.1
67.8	4.40	4.98	15.2	9.0	6.2
70.1	4.48	5.02	17.3	9.4	7.9
Nd ¹⁴⁶ (B ¹⁰ ,7n)Tb ^{149g}					
75.1	5.54	6.25	15.7	12.8	2.9
102.4	7.35	8.12	41.2	29.5	11.7
Nd ¹⁴⁶ (B ¹¹ ,8n)Tb ^{149g}					
90.2	5.10	5.83	17.8	14.6	3.2
103.7	6.50	7.29	30.3	26.3	4.0
112.8	6.94	7.80	38.8	32.8	6.0
Nd ¹⁴² (C ¹² ,3n)Dy ¹⁵¹					
55.6	3.61	4.11	9.3	5.0	4.3
70.1	4.11	4.66	22.6	8.2	14.4
Nd ¹⁴² (C ¹² ,4n)Dy ¹⁵⁰					
70.1	4.06	4.65	14.7	8.1	6.6
83.4	4.30	4.86	27.0	10.5	16.5
92.0	4.56	5.14	34.9	13.0	21.9
Nd ¹⁴² (C ¹² ,5n)Dy ¹⁴⁹					
83.4	4.20	4.78	16.8	10.1	6.7
92.0	4.36	4.93	24.7	11.9	12.8
100.6	4.48	5.06	32.7	13.7	19.0
111.7	4.81	5.44	42.9	17.5	25.4
122.8	5.22	5.87	53.1	22.5	30.6
Nd ¹⁴⁴ (C ¹² ,5n)Dy ¹⁵¹					
77.5	4.48	5.23	15.2	11.1	4.1
83.4	4.57	5.25	20.7	12.2	8.5
94.0	4.88	5.47	30.5	14.9	15.6
Nd ¹⁴⁴ (C ¹² ,6n)Dy ¹⁵⁰					
94.0	4.87	5.64	22.6	15.8	6.8
99.7	4.85	5.52	27.8	16.0	11.8
111.6	5.19	5.92	38.8	20.6	18.2
122.8	5.32	6.06	49.2	23.8	25.4
Nd ¹⁴⁴ (C ¹² ,7n)Dy ¹⁴⁹					
94.0	4.66	5.35	12.4	14.1	-1.7
99.7	4.68	5.39	17.6	15.2	2.4
111.6	5.03	5.74	28.6	19.3	9.3
122.8	5.09	5.84	39.0	21.9	17.1
Ce ¹⁴⁰ (O ¹⁶ ,5n)Dy ¹⁵¹					
89.7	3.63	4.16	15.4	11.0	4.4
101.0	3.78	4.27	25.5	13.0	12.5
111.0	3.95	4.55	34.5	16.1	18.4
Ce ¹⁴⁰ (O ¹⁶ ,6n)Dy ¹⁵⁰					
101.0	3.81	4.33	17.6	13.3	4.3
111.0	3.95	4.55	26.6	16.1	10.5
121.1	4.22	4.80	35.7	19.6	16.1
130.4	4.20	4.71	44.0	20.3	23.7
139.2	4.24	4.77	51.9	22.3	29.6
Ce ¹⁴⁰ (O ¹⁶ ,7n)Dy ¹⁴⁹					
111.0	4.20	4.76	16.4	17.8	-1.4
121.1	4.17	4.70	25.5	19.0	6.5
130.4	4.21	4.75	33.8	20.9	12.9
139.2	4.26	4.82	41.7	23.0	18.7
163.0	4.71	5.29	63.1	32.3	30.8

leads us to expect that most of the neutrons are emitted with nearly isotropic angular distributions.⁷ As shown in Sec. II, the value of $\langle\theta_L^2\rangle^{1/2}$ is not very sensitive to small anisotropies in neutron emission.

Let us assume initially that all neutrons are emitted isotropically. From Eqs. (13) and (15) we can calculate the average energy emitted as photons, and the average kinetic energy of the neutrons for each reaction. The results of these calculations are given in Table IV. First

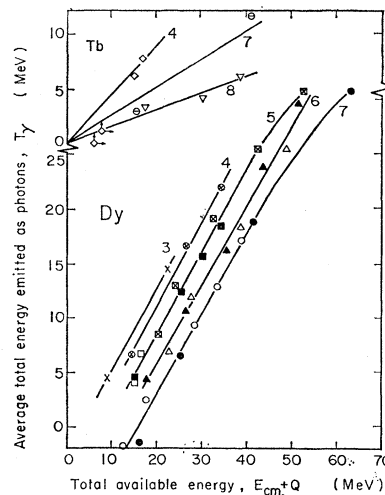


Fig. 5. Total photon energy versus total available energy. The upper curves are for Tb compound nuclei and the product Tb^{149g}. The lower curves are for Dy compound nuclei and products Dy¹⁴⁹, Dy¹⁵⁰, and Dy¹⁵¹. The number of emitted neutrons is indicated for each curve. Symbols are as follows:

- Pr¹⁴¹(C¹²,4n)Tb^{149g} \diamond ; Nd¹⁴⁶(B¹⁰,7n)Tb^{149g} \ominus ;
- Nd¹⁴⁶(B¹¹,8n)Tb^{149g} ∇ ; Nd¹⁴²(C¹²,3n)Dy¹⁵¹ \times ;
- Nd¹⁴²(C¹²,4n)Dy¹⁵⁰ \otimes ; Nd¹⁴²(C¹²,5n)Dy¹⁴⁹ \boxtimes ;
- Nd¹⁴⁴(C¹²,5n)Dy¹⁵¹ \square ; Nd¹⁴⁴(C¹²,6n)Dy¹⁵⁰ \triangle ;
- Nd¹⁴⁴(C¹²,7n)Dy¹⁴⁹ \circ ; Ce¹⁴⁰(O¹⁶,5n)Dy¹⁵¹ \blacksquare ;
- Ce¹⁴⁰(O¹⁶,6n)Dy¹⁵⁰ \blacktriangle ; Ce¹⁴⁰(O¹⁶,7n)Dy¹⁴⁹ \bullet .

we give the bombarding energy; then the average angles $\langle\theta_L\rangle$ and $\langle\theta_L^2\rangle^{1/2}$ corrected for target thickness and angular definition of the beam. In the last three columns we give the total available energy (Seeger's mass formula was used¹²), the average total kinetic energy of the neutrons, and average total photon energy. We estimate that the values of T_n have a standard error from experimental sources of not more than about 10%.

If the neutrons are not emitted isotropically, the true energies will differ from those given in Table IV. The maximum alteration due to this effect can be estimated from Eq. (10), which indicates that $\langle\theta_L^2\rangle$ for isotropic neutron emission is approximately 33% greater than for $W(\theta) \propto 1/\sin\theta$. Thus, if all the neutrons are emitted with this extremely anisotropic angular distribution, then the neutron kinetic energies should be increased by about 33% [see Eq. (15)]. Also, the total photon energies should be correspondingly decreased [see Eq. (13)]. In this paper we proceed with the discussion based on the approximation of isotropy. For this reason the neutron energies in Table IV are probably somewhat too small, and the photon energies are too large. Note that these errors are systematic. Therefore, they probably have only a small effect on the dependence of T_n and T_γ on reaction type and bombarding energy. Precise measurements of range straggling due to the velocity distribution would give a test of this approximation. [Compare Eqs. (4) and (9).]

¹² P. A. Seeger, Nucl. Phys. 25, 1 (1961).

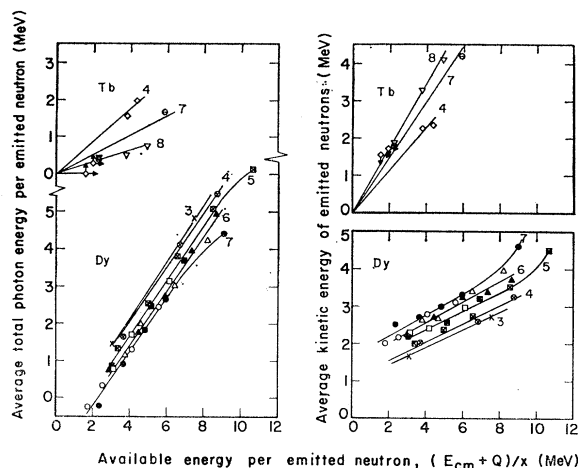


FIG. 6. Average total energy of photons (a) and average energy of neutrons (b) versus available energy per emitted neutron $(E_{c.m.} + Q)/x$ for reactions in which x neutrons are emitted. Symbols are as in Fig. 5.

In Fig. 5 we plot the average total photon energy T_γ against the total available energy.¹³ There is a striking difference between the (HI, xn) reactions (HI means heavy-ion induced) leading to Dy^{149} , Dy^{150} , Dy^{151} , and those leading to Tb^{149g} . Increasing the available energy leads to a rather slowly increasing photon energy for Tb^{149g} reactions. But for Dy reactions most of the available energy greater than about 10 or 15 MeV is dissipated by photon emission.

There is a small internal inconsistency in the T_γ values that we have calculated. These values become negative for two cases; this effect is on the border line of our experimental errors. Also, this result depends on the masses used to calculate Q values. We have Seeger's mass formula for both the target- and heavy-product nuclei.¹² If the angular distribution of the neutrons is peaked forward and backward, this inconsistency is even more pronounced.

As discussed in another paper, the reactions leading to Tb^{149g} probably involve only systems of low-angular momentum ($\lesssim 7.5\hbar$).¹ The results of this study imply that for these Tb compound nuclei of low-spin photon emission does not compete favorably with neutron emission. The reactions leading to Dy^{149} , Dy^{150} , and Dy^{151} have very high cross sections⁴; thus, the observed

¹³ The total photon energies that we have deduced may be compared with the results of Morton *et al.* (Ref. 5; see Table I in particular.) The comparisons cannot be made quantitatively because of differences in the experimental conditions and the method of analysis. We cannot calculate values of the root-mean-square angle from the data of Morton *et al.* because of their rather low-angular resolution. Their analysis involved a Monte Carlo calculation of the angular distribution with an adjustable parameter denoted by the symbol E_γ . In the Monte Carlo calculation the quantity E_γ was added to the Q value for the reaction. Thus, E_γ represents a part of the average total photon energy (T_γ). The values of E_γ from Ref. 5 can be compared with the values of T_γ in Fig. 5 by the relationship $E_\gamma + 5 \approx T_\gamma$ (except for energies near threshold). The consistency of this comparison of the two studies is very gratifying.

products must be formed from compound nuclei that have angular momentum distributions typical of most compound systems. Presumably, this primary angular-momentum distribution gives rise to a large number of compound nuclei of high spin.² As the excited nuclei decay, the angular momentum must be removed by particle and photon emission. Angular momentum barriers increase the lifetime for neutron emission, and, thus, photon emission becomes a competitive process. Grover has described the features of this competition.¹⁴

Another way of presenting our experimental results is to plot the average energies per emitted neutron versus the available energy per neutron $(E_{c.m.} + Q)/x$. These plots are shown in Fig. 6. Plots of cross section versus available energy per neutron lead to very similar results for these and other similar reactions. The reactions $(HI, xn)Dy^{149}$, Dy^{150} , Dy^{151} all peak at about 5.9 MeV per neutron.⁴ The reactions $(HI, xn)Tb^{149g}$ all peak at 3 to 4 MeV per neutron.¹

The Tb^{149g} reactions give values of T_n and T_γ that are expected from evaporation theory without angular-momentum effects. Increasing available energy goes mainly into kinetic energy of the neutrons. For Dy reactions the average kinetic energy of the neutrons increases rather slowly with available energy. For the smaller available energies almost no energy goes to photons. For the higher available energies the photon and neutron energies are comparable.

It has frequently been assumed that the classical rotational energy of a compound nucleus is not available for nuclear evaporation.¹⁵ Thus, this rotational energy is expected to be dissipated by additional photon emission. Such an effect is not apparent from the angular distribution results. The reactions of C^{12} with Nd^{144} and of O^{16} with Ce^{140} both form Dy^{156} compound nuclei. Over the energy region of our studies, the average squares of the angular momenta differ by about 25% for a given value of the excitation energy. And yet, in Figs. 5 and 6, the values of T_n and T_γ are usually indistinguishable. (A possible exception is for Dy^{149} production at energies near threshold.) The relationship between average total photon energy and angular momentum is discussed further in the preceding paper.⁴

These values of average neutron and photon energies are associated with specific reactions involving neutron emission. Mollenauer's observations⁶ of photons are, on the other hand, not associated with such specific reactions. By reference to the excitation functions, we can extract information about average energies of all neutron-emitting reactions. Excitation functions for all the $(HI, xn)Dy^{149}$, Dy^{150} , Dy^{151} reactions peak at about 5.9 MeV per emitted neutron.⁴ Thus, if we compare T_n and T_γ values at 5.9 MeV per neutron, we get a measure of the variation of these quantities with number (x) of

¹⁴ J. R. Grover, Phys. Rev. **127**, 2142 (1962); **123**, 267 (1961).

¹⁵ G. A. Pik-Pichak, Zh. Eksperim. i Teor. Fiz. **38**, 768 (1960) [translation: Soviet Phys.—JETP **11**, 557 (1960)].

neutrons or excitation energy (E). The values of the average neutron energy (at 5.9 MeV per neutron) in Fig. 6 are proportional to $(E)^{0.4 \pm 0.15}$. This relationship reflects the increase in nuclear temperature with excitation energy. The excitation functions give information related to the energy and angular momentum of the first neutron emitted in the evaporation chain. A more detailed comparison of the results of this study with excitation function measurements is given in the following paper.⁴

C. Conclusions

To summarize this study we may list the following conclusions: (a) The reactions involving neutron emission that lead to Dy^{149} , Dy^{150} , and Dy^{151} proceed by compound-nucleus formation. (b) The energetics of the decay of Dy^{156} (excited to 65 to 125 MeV) to Dy^{149} , Dy^{150} , and Dy^{151} are almost the same for $C^{12}+Nd^{144}$ and for $O^{16}+Ce^{140}$ in spite of a difference of about 25% in $\langle J^2 \rangle$. (c) Compound nuclei of low spin (as measured by reactions forming Tb^{149g}) have very different decay

properties from those of high spin (as measured by reactions forming Dy^{149} , Dy^{150} , and Dy^{151}). (d) The low-spin compound systems dissipate less than about 12 MeV in photons; the remaining energy appears as kinetic energy of the emitted neutrons. (e) The compound systems of higher spin dissipate, on the average, about one-half their available excitation energy by photon emission. (f) For a given reaction, the average total photon energy (T_γ) increases almost linearly with the available energy, and extends to T_γ values of approximately 30 MeV for available energies of 50 to 60 MeV. (g) The average kinetic energy of the neutrons increases approximately as the square root of the excitation energy.

ACKNOWLEDGMENTS

Dan O'Connell and Gordon Steers did a fine job of preparing targets. The HILAC crew worked hard to get a beam through two $\frac{1}{8}$ -in. collimators. We thank L. Altman, J. R. Grover, B. G. Harvey, and E. K. Hyde for reading the manuscript.

Inelastic Scattering of 10.2-MeV Protons by $N^{14}\dagger$

P. F. DONOVAN

*Bell Telephone Laboratories, Inc., Murray Hill, New Jersey, and
Brookhaven National Laboratory, Upton, New York*

AND

J. F. MOLLENAUER AND E. K. WARBURTON

Brookhaven National Laboratory, Upton, New York

(Received 8 August 1963)

The inelastic scattering of protons from N^{14} was studied at an incident proton energy of 10.2 MeV. Proton groups were observed corresponding to all the well-established N^{14} states below 8.0 MeV. No evidence was obtained for the levels at 7.60, 7.40, 6.60, and 6.05 MeV which were previously reported in this reaction. Angular distributions and total cross sections were measured for inelastic scattering to the N^{14} states between 3.95 and 7.03 MeV. The relative cross sections are found to be in rather good agreement with shell-model predictions.

I. INTRODUCTION

THE present investigation of the inelastic scattering of protons from N^{14} was undertaken for two reasons. First, previous work on this reaction was done at $E_p=9.5$ MeV by Burge and Prowse¹ using photographic emulsions to detect the scattered protons. These authors reported levels in N^{14} at 7.60 ± 0.02 , and 7.40 ± 0.02 MeV, and probable levels at 6.60 ± 0.04 and 5.95 MeV, in addition to the well-known levels² below

7-MeV excitation in N^{14} . Later, Hossian and Kamal³ reported results from reading of emulsions which were a part of the same series of exposures used by Burge and Prowse.¹ Hossian and Kamal reported levels in N^{14} at 6.05 ± 0.02 and 6.75 ± 0.03 MeV in addition to the well-known levels. One purpose of the present work, then, was to study the proton spectrum from $N^{14}(p, p')N^{14}$ at a proton energy close to that of the previous work as a check on the existence of N^{14} levels near 7.6, 7.4, 6.7, and 6.0 MeV.

The second reason for undertaking this study was to obtain relative cross sections for excitation of the N^{14}

[†] Work performed in part under the auspices of the U. S. Atomic Energy Commission.

¹ E. J. Burge and P. J. Prowse, *Phil. Mag.* **1**, 912 (1956).

² F. Ajzenberg-Selove and T. Lauritsen, *Nucl. Phys.* **11**, 1 (1959).

³ A. Hossian and A. N. Kamal, *Indian J. Phys.* **31**, 553 (1957).